

Determination of the Cs distribution along a line of sight by the Zeeman splitting in an inhomogeneous magnetic field

Christian Wimmer, M. Lindauer, Ursel Fantz

Angaben zur Veröffentlichung / Publication details:

Wimmer, Christian, M. Lindauer, and Ursel Fantz. 2018. "Determination of the Cs distribution along a line of sight by the Zeeman splitting in an inhomogeneous magnetic field." *Journal of Physics D: Applied Physics* 51 (39): 395203.
<https://doi.org/10.1088/1361-6463/aad93d>.

PAPER • OPEN ACCESS

Determination of the Cs distribution along a line of sight by the Zeeman splitting in an inhomogeneous magnetic field

To cite this article: C Wimmer *et al* 2018 *J. Phys. D: Appl. Phys.* **51** 395203

View the [article online](#) for updates and enhancements.

Related content

- [Towards powerful negative ion beams at the test facility ELISE for the ITER and DEMO NBI systems](#)
U. Fantz, C. Hopf, D. Wunderlich *et al.*
- [Towards large and powerful radio frequency driven negative ion sources for fusion](#)
B Heinemann, U Fantz, W Kraus *et al.*
- [Influence of the magnetic field topology on the performance of the large area negative hydrogen ion source test facility ELISE](#)
D Wunderlich, W Kraus, M Fröschle *et al.*

Recent citations

- [Measurement of the Magnetic Field in a Linear Magnetized Plasma by Tunable Diode Laser Absorption Spectroscopy](#)
Sven Dickheuer *et al*



IOP | ebooks™

Bringing you innovative digital publishing with leading voices to create your essential collection of books in STEM research.

Start exploring the collection - download the first chapter of every title for free.

Determination of the Cs distribution along a line of sight by the Zeeman splitting in an inhomogeneous magnetic field

C Wimmer[✉], M Lindauer and U Fantz

Max-Planck-Institut für Plasmaphysik, Boltzmannstr. 2, 85748 Garching, Germany

E-mail: christian.wimmer@ipp.mpg.de

Received 19 April 2018, revised 20 July 2018

Accepted for publication 9 August 2018

Published 23 August 2018



Abstract

Large-scale sources for negative hydrogen ions are required for the neutral beam injection of the ITER fusion device. Caesium is used for the conversion of hydrogen atoms into negative ions. The combination of moderate background vacuum conditions (10^{-7} – 10^{-6} mbar), the high reactivity of Cs, continuous evaporation of Cs and plasma-enabled redistribution of Cs and Cs^+ forms a complex dynamics. ELISE (extraction from a large ion source experiment) is a half ITER-source scale experiment. A tunable diode laser absorption spectroscopy (TDLAS) diagnostic at the resonant Cs $6^2\text{S}_{1/2}$ – $6^2\text{P}_{3/2}$ transition (852 nm) has been applied to the source in order to measure the density of neutral Cs close to the conversion surface and thus gaining a better insight into the Cs dynamics. An inhomogeneous magnetic field created by permanent magnets (≈ 25 – 320 G) is located along the line-of-sight (LOS) of the TDLAS, leading to a varying effect of the Zeeman splitting of the concerning Cs states and thus the absorption line profile along the LOS. In long plasma pulses at ELISE, a change of the Cs absorption line profile takes place, which can be attributed to a variation of the Cs density profile along the LOS. In order to attribute a measured line profile to a certain magnetic field strength and thus a certain position along the LOS, absorption spectra with a defined B-field at a Cs vapor cell using the same diagnostic system have been measured. The strong broadening of the measured line profile at ELISE after several 10 s of plasma indicates that neutral Cs is mainly located in the area of high magnetic field strength, i.e. close to the side wall. A correlation between the measured Cs density and the source performance exists during the beginning of the pulse and is lost in this later phase.

Keywords: negative hydrogen ion source, Zeeman splitting, tunable diode laser absorption spectroscopy, caesium dynamics

(Some figures may appear in colour only in the online journal)

1. Introduction

Caesium is used in large-scale sources for negative hydrogen ions, which are required for the neutral beam injection (NBI) of the ITER fusion device, for the sufficient production of D^- or H^- at low pressure ($p \leq 0.3$ Pa). One NBI beamline at

ITER needs to deliver an accelerated current of 40 A equivalent of 1 MeV D atoms (or 46 A equivalent of 870 keV H atoms) for a duration of up to one hour [1, 2]. Taking into account losses during the beam transport and neutralization, the ion source needs to deliver an extracted current density of $286 \text{ A m}^{-2} \text{ D}^-$ or $329 \text{ A m}^{-2} \text{ H}^-$ from an extraction area of 0.2 m^2 . ELISE (extraction from a large ion source experiment) is a 1/2 ITER source size test facility at IPP (Max-Planck-Institut f. Plasmaphysik) Garching that shall demonstrate the feasibility of the ITER requirements [3]. Full size sources



Original content from this work may be used under the terms of the [Creative Commons Attribution 3.0 licence](https://creativecommons.org/licenses/by/3.0/). Any further distribution of this work must maintain attribution to the author(s) and the title of the work, journal citation and DOI.

are under construction at Consorzio RFX, Padova [4]. The working principle of such ion sources is the following:

A low-pressure, low-temperature hydrogen plasma ($T_e \approx 10$ eV [5]) is created in several cylindrical drivers (4 at ELISE, 8 at the ITER sources) by inductive RF coupling with a power of up to 90 kW per driver. The plasma expands from the drivers into one common expansion chamber, in which a magnetic filter field (order of several 10 G) is applied to cool the plasma down to an electron temperature of $T_e \approx 1$ eV. The reduced electron temperature is mandatory in order to lower the destruction of negative ions by electron stripping. Negative hydrogen ions are created by surface conversion [6] of mainly hydrogen atoms [7] on the plasma grid (PG), which is the first grid of the extraction and acceleration system. For achieving a high conversion yield, a low work function of the conversion surface is mandatory. For this reason, Cs (work function of 2.1 eV) is evaporated into the source.

The dynamics of Cs in the source is complex: during operation, Cs is continuously evaporated from several ovens (two at ELISE). Due to moderate vacuum conditions (background pressure in the order of 10^{-7} – 10^{-6} mbar, being far from ultra high vacuum conditions), the highly reactive Cs forms compounds with residual gas vacuum impurities. A certain flux of elemental Cs onto the conversion surfaces needs to be delivered in order to maintain a layer of elemental Cs and thus achieve a stable, homogeneous low work function. Additionally, Cs is redistributed during plasma phases by the interaction of the plasma with Cs layers on the chamber surfaces [8, 9]. A large fraction of Cs is ionized during the plasma pulses due to the low ionization energy of Cs (3.89 eV). Unfortunately, ionized Cs is hard to access for diagnostics. For this reason, only the behavior of neutral Cs is investigated experimentally up to now in negative hydrogen ion sources. Nevertheless, the stability of the H_β emission during a discharge (being dependent on the electron density and temperature in addition to further parameters [10]) indicates that the ionization degree of Cs is fairly constant.

Since electrons form the minority species in the ion–ion plasma close to the extraction system [11], a small change of the H^- production yield can significantly change the electron fraction in the plasma and thus the co-extracted electron current. For this reason, the latter reacts usually more sensitive on the work function of the conversion surfaces and thus on the Cs coverage. Co-extracted electrons are a general issue in negative ion sources, since their thermal load of up to several 10 MW m^{-2} (they are removed out of the beam by magnets in the second grid) limits their tolerable amount to $j_e/j_{H^-} < 1$ for the ITER-source. The instability of the co-extracted electron current in long pulses is at the moment limiting the performance of the ELISE source [11, 12]. Thus, the presence of Cs in the central part close to the convertor surface is of high relevance in order to achieve a sufficiently stable Cs coverage and thus stable operation during long pulses of negative hydrogen ion sources. A deeper investigation of insight into the Cs dynamics close to the convertor surface is mandatory in order to understand the instability of electrons during long pulses and thus in order to reach the nominal ion current.

For the determination of the neutral Cs density in the ground state close to the convertor surface, a tunable diode laser

spectroscopy (TDLAS) at the resonant Cs 852 nm transition ($6^2S_{1/2} \rightarrow 6^2P_{3/2}$, named Cs-D2) is applied at ELISE, measuring the hyperfine spectrum. The density of Cs^0 in the ground state reflects the total density of neutral Cs, because the densities in the excited states contribute with less than 1% to the total population [13, 14]. Significant broadening and distortion of the lines result from the Doppler effect as well as from the Zeeman effect; further broadening mechanisms as the pressure or Stark broadening are of no relevance in the ion sources. Two different magnetic filter field setups are in use at ELISE, for which the magnetic field topology differs significantly along the line-of-sight (LOS) of the TDLAS diagnostic: in the standard setup, the filter field is solely created by a vertical current through the PG in the range of several kA, resulting in a widely homogeneous field strength of several 10 G along the LOS (typical length ≈ 1 m). In the second setup, the magnetic field topology is modified by adding bars of permanent magnets externally to the source, leading to an inhomogeneous magnetic field strength along the LOS with a peak strength of several 100 G close to the side wall. In particular at these higher field strengths, the Zeeman splitting of the $6^2S_{1/2}$ and $6^2P_{3/2}$ states leads to a distortion of the absorption line profile. The effect of the Zeeman splitting on the absorption spectrum of Cs has been used in order to gain a certain spatial resolution of the Cs distribution along the LOS.

2. Structure of the Cs $6^2S_{1/2}$ and $6^2P_{3/2}$ states

The effect of the magnetic field strength on the relative energy of the Cs $6^2S_{1/2}$ ground state and $6^2P_{3/2}$ excited state is shown in figure 1. Without B-field, the $6^2S_{1/2}$ state is hyperfine-split into two levels (with the total angular momentum quantum number of the atom $F = 3, 4$). The $6^2P_{3/2}$ state splits into four levels ($F = 2, 3, 4, 5$). The selection rule ($\Delta F = -1, 0, +1$) gives 6 transitions, at which each three overlap at relevant Doppler temperatures resulting in two resolvable peaks [16]. The presence of a magnetic field brakes the degeneracy of each hyperfine level into $2F + 1$ sub-levels with magnetic quantum number $m_F = -F, -F + 1, \dots, +F$. This splitting is symmetric at low field (Zeeman regime) and a strong shift of the levels occurs at high field strength (Paschen–Back regime, starting at ≈ 100 G for the $6^2P_{3/2}$ state and at several 1000 G for the $6^2S_{1/2}$ state). Whereas in the Zeeman-regime the levels are still grouped by F , the levels are grouped by the total magnetic quantum number m_J in the Paschen–Back regime. The additional selection rule $\Delta m_F = -1, 0, +1$ (σ^-, π, σ^+ transitions) results in a complex structure of 126 Doppler-broadened lines. The wavelength position of these lines is shown in figure 2 for 100 G and 400 G [15, 17, 18].

3. Absorption line profiles at a Cs vapor cell with varying B-field

In order to determine experimentally the effect of the magnetic field on the measured absorption spectrum, measurements at a Cs vapor cell, which has been positioned at varying

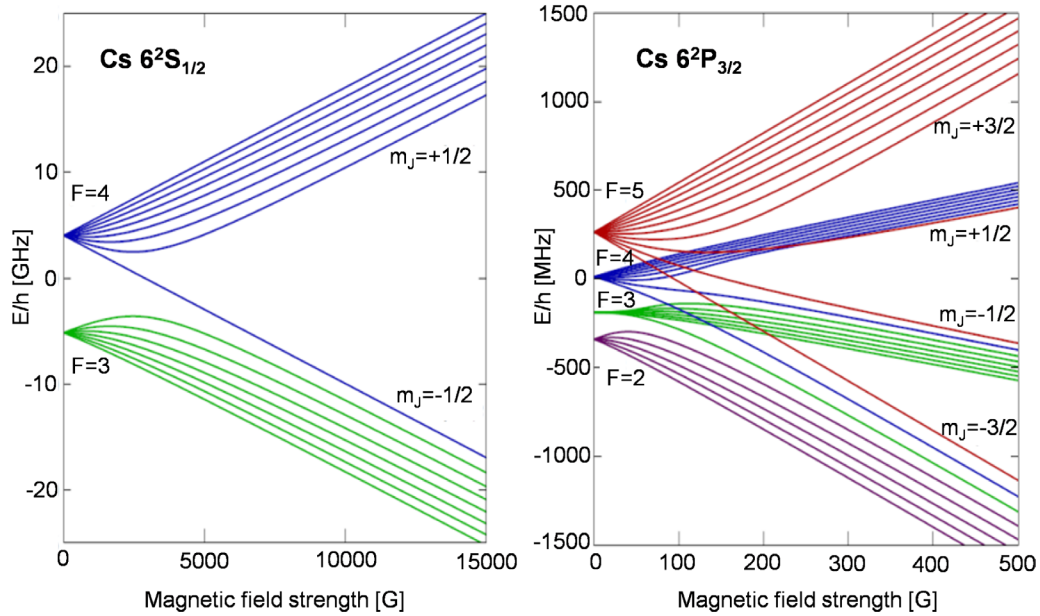


Figure 1. Splitting of the Cs $6^2S_{1/2}$ ground state (left) and $6^2P_{3/2}$ state (right) as function of the magnetic field strength. Both axis are scaled differently for the $6^2S_{1/2}$ and $6^2P_{3/2}$ state [15]. Reproduced with permission from [15]. Copyright © 1998, by Daniel Adam Steck. All rights reserved.

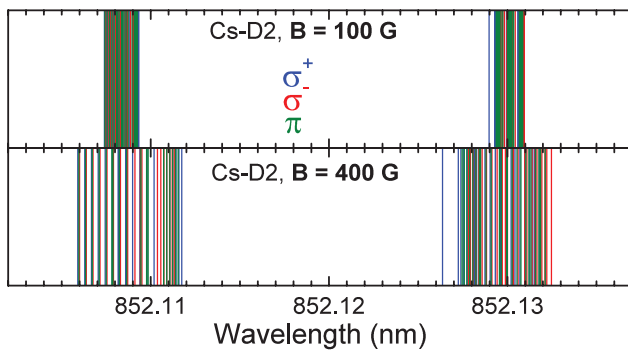


Figure 2. Wavelength (in air) of the individual Zeeman-split Cs-D2 transition lines for a magnetic field strength of 100 G (top) and 400 G (bottom).

distance to a bar of permanent magnets, have been carried out using the same diagnostic setup as at the ELISE source. The experimental setup is shown in figure 3(a). As light source, a single-frequency, multimode fiber-coupled distributed feedback diode laser (Sacher Lasertechnik, DFB LQ5i-852-16) is used. It delivers an output power of up to 20 mW and can be tuned around the Cs-852 nm transition without mode hops by current tuning. Typically, the tuning speed is chosen to record ten spectra per second. Its output linewidth (1.5 MHz) is much lower than the Doppler broadening at room temperature (several 100 MHz), thus the Doppler-broadened spectrum is well resolved. In front of the Cs vapor cell (diameter of 19 mm), an aspheric lens (focal length of 25 mm) creates a line-of-sight (LOS) with a diameter of ≈ 1 cm. A neutral density (ND) filter damps the light about 2 orders of magnitude in order to avoid depopulation of the Cs ground state at high light intensity [16]. The light is collimated by a similar lens into a multimode fiber and the intensity is recorded with an amplified photo diode (Thorlabs PDA36A). An interference filter (central wavelength 852 nm, $\Delta\lambda_{FWHM} = 10$ nm) is used in order

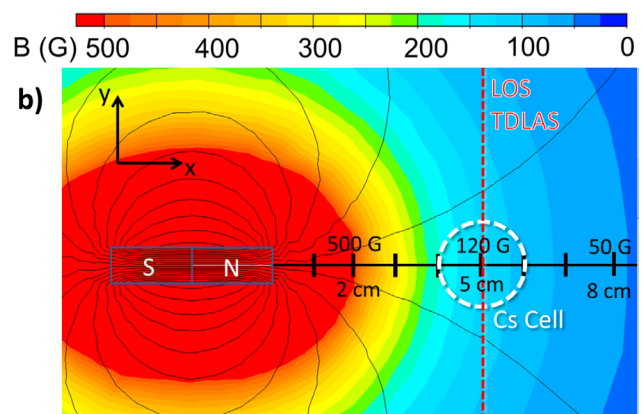
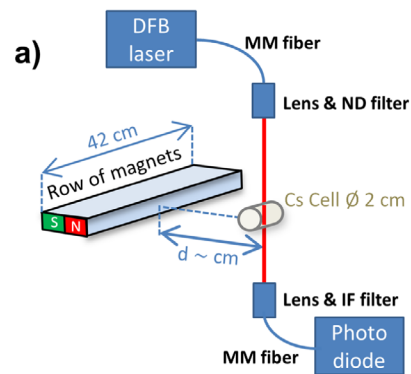


Figure 3. (a) Experimental setup for the measurement of absorption spectra in a Cs vapor cell with a magnetic field created by a bar of permanent magnets. (b) Magnetic field map of the setup.

to filter ambient light causing an offset on the photo diode signal. The wavelength calibration of the recorded spectra is carried out using the two positions of the recorded absorption peaks assuming linear dependence between the diode laser current and the output wavelength.

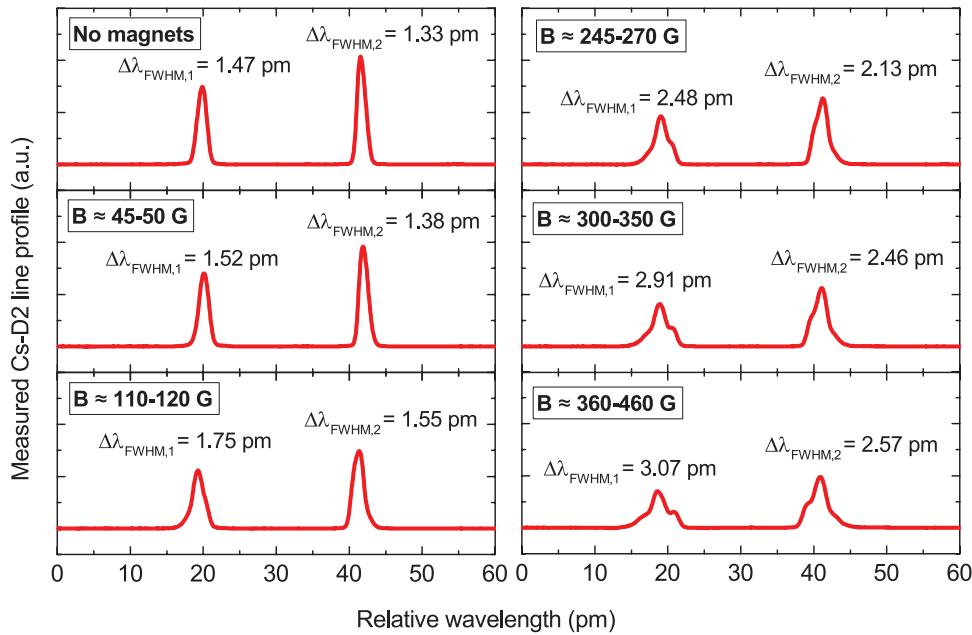


Figure 4. Cs-D2 absorption line profiles recorded at the Cs vapor cell without magnetic field and at different magnetic field strengths. The FWHM of each peak is given, resulting from a Gaussian fit.

A bar of permanent magnets (CoSm magnets with a total size of $3.9 \times 0.9 \times 42 \text{ cm}^3$) can be positioned at variable distance to the Cs vapor cell. A 2D plot of the resulting magnetic field strength (calculated with QuickField) is shown in figure 3(b). The whole setup is kept at room temperature, where the vapor pressure of Cs creates a Cs density in the order of 10^{16} m^{-3} inside the Cs vapor cell [19].

The measured absorption line profiles $-\ln [I(\lambda)/I_0(\lambda)]$, $I(\lambda)$ denoting the light intensity after passing the absorption medium and $I_0(\lambda)$ before the absorption medium, are shown in figure 4 for six different magnetic field strengths up to $\approx 400 \text{ G}$. The relative wavelength axis results from the tuning of the used diode laser. Due to temperature drifts, the zero point might not correspond to the same absolute wavelength in the figures 4 and 7. The line shape of the two resolvable peaks (both consisting of three overlapped hyperfine lines without B-field) is perfectly Gaussian due to the dominating Doppler broadening in case of no B-field and still pretty Gaussian in case of 45–50 G and 110–120 G, and the linewidth is increasing with increasing B-field, attributed to the symmetric splitting of the $6^2S_{1/2}$ ground state and $6^2P_{3/2}$ excited state in the Zeeman-regime (compare to figure 1). At stronger field strength, the recorded spectra are no longer Gaussian and in particular at the strongest B-field (360–460 G) both peaks show a strong distortion, created by the mixture of Zeeman-regime of the $6^2S_{1/2}$ and hyperfine Paschen–Back regime of the $6^2P_{3/2}$ state.

4. Absorption line profiles in an inhomogeneous B-field at the ELISE test facility

Figure 5 shows a sketch of the ELISE ion source. A hydrogen plasma is created in four drivers by inductive RF coupling with a total available RF power up to 300 kW. The positions of

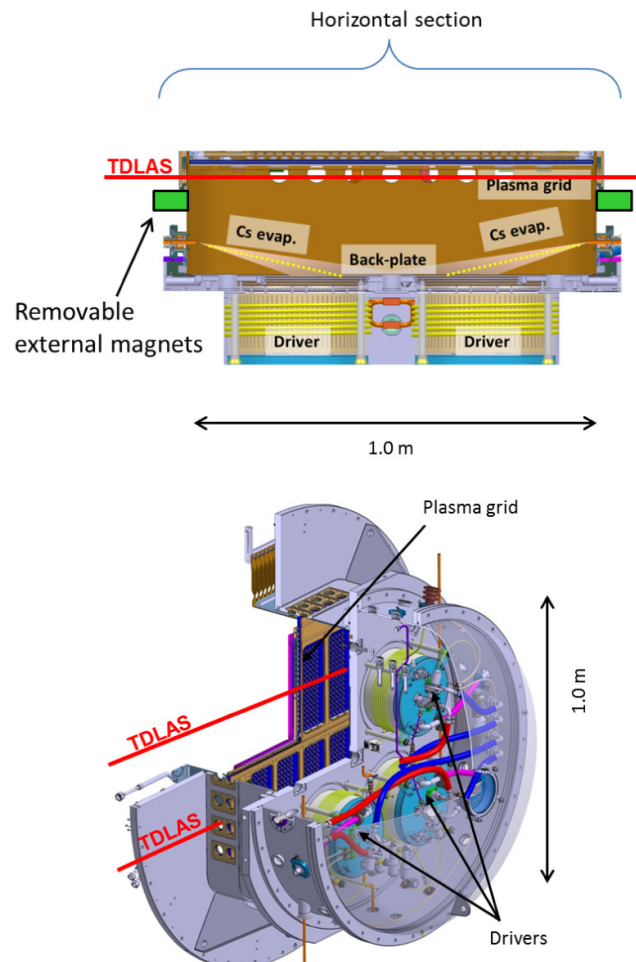


Figure 5. Top: horizontal cut through the ion source of ELISE. The positions of the Cs ovens as well as the axial position of the TDLAS measurement are indicated. Bottom: view of the ELISE ion source from the back with the two LOS for TDLAS.

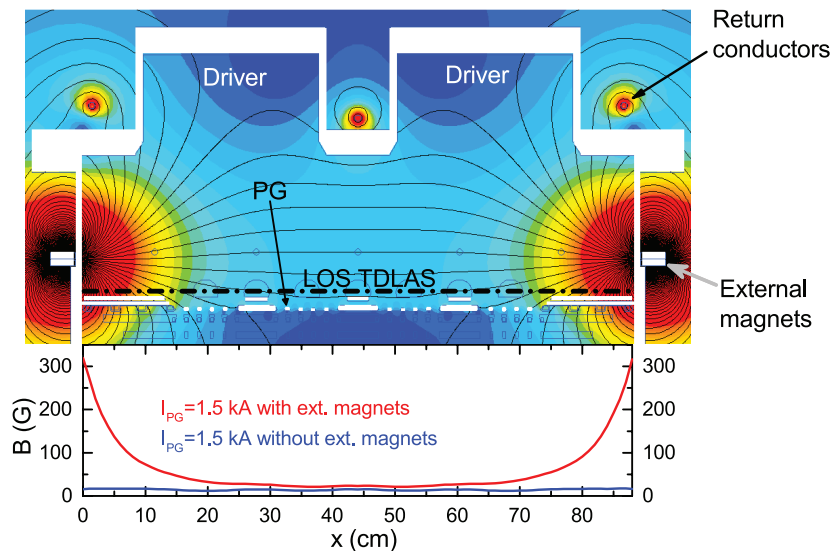


Figure 6. 2D plot of the magnetic field topology at ELISE with external magnets and the total magnetic field strength along the LOS of TDLAS for a PG current of 1.5 kA, with and without external magnets.

the external magnets (similar bars as used at the Cs vapor cell) at the side walls are indicated. The particle beam is extracted through 640 apertures of 14 mm diameter, which are arranged in eight beamlet groups of 80 apertures each. For extraction and acceleration of the beam, high voltage of up to -60 kV is applied to the source using a typical extraction voltage of 10 kV between PG and the second grid (extraction grid). The third grid is grounded. ELISE is capable to demonstrate plasma pulses with the full length of the ITER requirements (up to one hour); however, due to technical limitations of the HV supply, a particle beam can only be extracted for 10 s every three minutes within a plasma pulse (called beam extraction blips). Consecutive plasma pulses are divided by a vacuum phase of several minutes. For the evaporation of Cs, two Cs ovens are mounted at the side wall of the expansion chamber. During operation, Cs is continuously evaporated through two nozzles, which direct the Cs flow towards the back plate of the expansion chamber, as indicated in figure 5. In order to avoid a strong local adsorption of Cs, all walls of the ion source are controlled to a temperature of 45 °C. The PG as well as the bias plate, which covers the PG outside of the beamlet groups, is kept at a higher temperature of typically 125 °C. A more detailed description of ELISE can be found elsewhere [3, 11].

For the measurement of the Cs density, the TDLAS diagnostic described before is installed at two horizontal lines of sight (LOS) in the top and bottom part of the source (vertically in the center of the driver projection) at an axial distance of 2 cm to the plasma grid. It allows for the measurement of the LOS-averaged neutral Cs density (length of LOS: 0.875 m, diameter ≈ 1 cm). In the following, only measurements from the bottom LOS will be presented—however, all results are also valid for the top LOS.

A 2D plot of the magnetic field topology as well as the field strength along the LOS of TDLAS with and without external magnets (both using a PG current of 1.5 kA) is shown in figure 6. The external magnets are placed with their polarity strengthening the regular B-field. Without

external magnets, the B-field is pretty homogeneous along the LOS with a value of ≈ 15 G. The external magnets lead to a peaking B-field close to the side wall (up to ≈ 320 G), whereas in the central area the B-field is weakly increased to a value of ≈ 20 – 25 G [20].

In the following, absorption line profiles from two ELISE pulses with and without external magnets are compared. Four line profiles of each pulse are shown in figure 7. The plasma was ignited at $t = 1.2$ s and the RF power has been turned off at $t = 202.2$ s. In the vacuum phase before the RF pulse, the Gaussian-shaped absorption peaks in case of ‘without external magnets’ result in a Doppler temperature of 350 ± 50 K. This fits very well to the temperature of the source walls (320 K) and of the Cs oven (550 K). For the evaluation of the Doppler temperature, only the hyperfine structure and no effect of the Zeeman splitting is taken into account. In case of ‘with external magnets’ the FWHM of both peaks is slightly increased by approximately 20%. More significant is the difference during the plasma phase: comparing the spectra at $t = 200$ s, the evaluated temperature in case of ‘without external magnets’ results in 960 ± 100 K, which is in agreement with the gas temperature of hydrogen in the source (0.1 eV [10]). With the external magnets, the FWHM of the peaks are increased by more than 70% caused by the Zeeman splitting. The different further broadening of the peaks by the external magnets between vacuum and plasma phase gives already a hint of a different spatial distribution of neutral Cs in these two phases.

Comparing TDLAS data of homogeneous and heterogeneous B-field distributions can reveal inhomogeneities of the Cs distribution along the LOS. Cs situated close to the side walls of the source chamber will show a strong Zeeman splitting in case of the mounted external magnets, while Cs atoms in the more central part of the LOS will be characterized by a weak Zeeman splitting. The much increased FWHM of the absorption peaks with mounted external magnets during plasma indicates that a large fraction of the measured neutral Cs is located in areas with high field strength ($\gtrsim 100$ G,

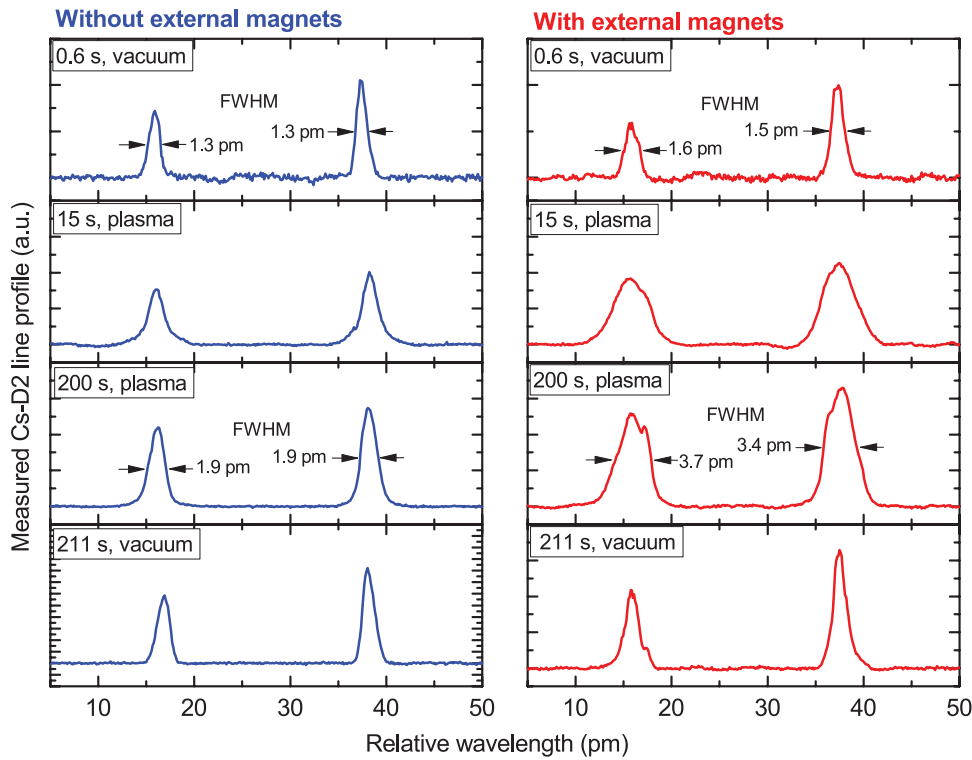


Figure 7. Absorption line profiles recorded at the ELISE test facility in the vacuum phase before the pulse (top), after the pulse (bottom) and during the pulse (center). Left: without external magnets. Right: with external magnets.

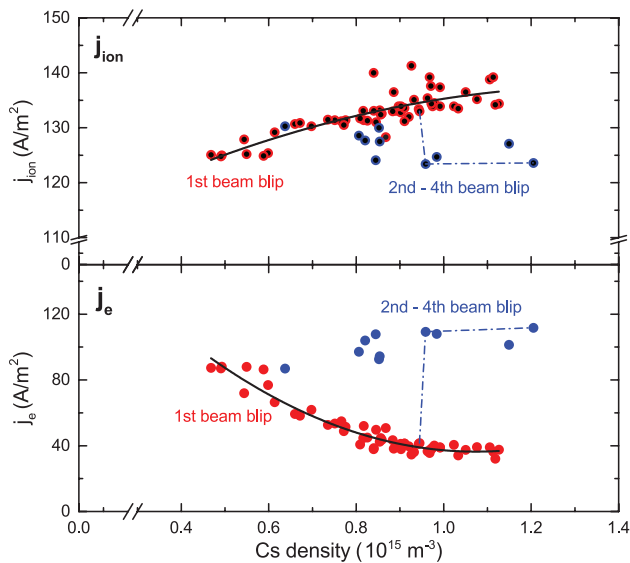


Figure 8. Extracted current densities j_{ion} and j_e as function of the measured Cs density during Cs conditioning of ELISE, distinguished between the first beam extraction blip of a pulse (red) and later extraction blips (blue). The evolution of one pulse containing three beam blips is indicated by the dashed line.

i.e. several cm close to the side wall). Of particular interest is the transition of the peak shape from $t = 15$ s to $t = 200$ s: whereas at $t = 15$ s the peak shape is fairly Gaussian, a clear distortion of the peak created in the mix of Zeeman regime of the $6^2S_{1/2}$ state and hyperfine Paschen–Back regime of the $6^2P_{3/2}$ state is to be seen in the spectrum at $t = 200$ s (in fact, it appears already after a time of several 10 s). Comparing the

spectrum to the measurements at the Cs vapor cell (figure 4), it can be stated that almost all neutral Cs along the LOS is located at positions with high B-field ($\gtrsim 300$ G) and thus very close to the side wall at $t = 200$ s. In contrary, the full distortion of the mixed regime is not yet seen at $t = 15$ s, indicating that a certain fraction of neutral Cs is located at lower magnetic field strength, i.e. more in the central part of the LOS closer to the beamlet groups of the plasma grid, filling the dip in the pure spectrum of the mixed regime. This fraction of neutral Cs is, however, obviously depleted during the pulse.

This depletion of neutral Cs in the central part of the LOS has an impact on the correlation between the extracted current densities and the measured Cs density: plotted in figure 8 is the extracted negative deuterium ion current j_{ion} and co-extracted electron current j_e as function of the measured neutral Cs density for several consecutive pulses during a Cs conditioning phase of the ELISE source. All values are averaged during the second half, i.e. 5 s, of the extraction phase (beam blip). Most of the pulses have been short (20 s plasma) including only one beam extraction blip, but also some longer pulses (up to 590 s plasma, including four beam extraction blips) have been carried out. As mentioned in the introduction and regularly seen [11], the co-extracted electron current density shows a higher dynamic during the conditioning than the negative ions.

Both extracted current densities (j_e more pronounced) show a clear correlation with the measured neutral Cs density—this correlation is, however, only valid for the first beam blip and is lost from the second beam blip onwards. This is in agreement to the fact that in this later phase no significant amount of the measured Cs is located in the central part of the LOS close to the beamlet groups of the plasma grid, where

it is required for the formation of stable Cs layers. The Cs mainly situated close to the side walls from the second beam extraction blip onwards does not contribute to build up and maintain these layers. Techniques for achieving a sufficient flux of Cs onto the PG in long pulses need to be found.

5. Conclusion

The distortion of Doppler-broadened absorption line profiles of the Cs-D2 transition by the Zeeman effect in a magnetic field has been used to gain a certain amount of spatial resolution along a LOS with inhomogeneous magnetic field strength in the ELISE test facility. The appearance of a clearly distorted spectrum after several 10 s of plasma time clearly indicates that almost all measured neutral Cs is located in regions with high field strength, i.e. close to the side walls and therefore Cs is depleted in the central part close to the beamlet groups of the plasma grid. This depletion is in agreement with measurements indicating a correlation between the extracted current densities and the measured Cs density during the beginning of a pulse, but not later during the pulse. However, achieving a sufficient Cs flux onto the plasma grid for achieving stable Cs layers and thus a stable performance in long pulses is highly aimed for the negative hydrogen ion sources for the ITER neutral beam injectors.

Acknowledgments

The authors would like to thank the whole IPP NNBI-team and in particular Markus Fröschle for their input and help.

ORCID iDs

C Wimmer  <https://orcid.org/0000-0003-4691-4265>

References

- [1] ITER 2011 Neutral beam heating and current drive system design description document (DDD) 5.3
- [2] Hemsworth R *et al* 2009 *Nucl. Fusion* **49** 045006
- [3] Heinemann B *et al* 2009 *Fusion Eng. Des.* **84** 915
- [4] Toigo V *et al* 2017 *New J. Phys.* **19** 085004
- [5] Fantz U, Schiesko L, Wunderlich D and NNBI Team 2013 *AIP Conf. Proc.* **1515** 187
- [6] Bacal M and Wada M 2015 *Appl. Phys. Rev.* **2** 021305
- [7] Wunderlich D, Gutser R and Fantz U 2009 *Plasma Sources Sci. Technol.* **18** 045031
- [8] Wimmer C, Fantz U and NNBI-Team 2013 *AIP Conf. Proc.* **1515** 246
- [9] Mimo A, Wimmer C, Wunderlich D and Fantz U 2017 *AIP Conf. Proc.* **1869** 030019
- [10] Fantz U, Falter H, Franzen P, Wunderlich D, Berger M, Lorenz A, Kraus W, McNeely P, Riedl R and Speth E 2006 *Nucl. Fusion* **46** S297
- [11] Heinemann B, Fantz U, Kraus W, Schiesko L, Wimmer C, Wunderlich D, Bonomo F, Fröschle M, Nocentini R and Riedl R 2017 *New J. Phys.* **19** 015001
- [12] Wunderlich D, Fantz U, Heinemann B, Kraus W, Riedl R, Wimmer C and The NNBI Team 2016 *Nucl. Fusion* **56** 106004
- [13] Wunderlich D, Wimmer C and Friedl R 2014 *J. Quant. Spectrosc. Radiat. Transfer* **149** 360–71
- [14] Priti P, Dipti D, Gangwar R and Srivastava R 2017 *J. Quant. Spectrosc. Radiat. Transfer* **187** 426–42
- [15] Steck D A 2010 Cesium D Line Data revision 2.1.4 (<http://steck.us/alkalidata>)
- [16] Fantz U and Wimmer C 2011 *J. Phys. D: Appl. Phys.* **44** 335202
- [17] Arimondo E, Inguscio M and Violino P 1977 *Rev. Mod. Phys.* **49** 31–75
- [18] Belin G, Holmgren L and Svanberg S 1976 *Phys. Scr.* **14** 39
- [19] Taylor J B and Langmuir I 1937 *Phys. Rev.* **51** 753
- [20] Wunderlich D, Kraus W, Fröschle M, Riedl R, Fantz U, Heinemann B and The NNBI Team 2016 *Plasma Phys. Control. Fusion* **58** 125005